1. Introduction

Unique properties of phosphate based glasses, such as low melting temperature, low glass transition temperature, high transparency for ultraviolet (UV) light, low dispersion or relatively high refractive indices compared to silicate based glasses make them attractive for various technological applications like optical devices, hermetic seals, organic/inorganic composites, biomaterials, solid state electrolytes or materials for immobilization of nuclear waste [1, 2]. Special attention is paid to phosphate materials modified with transitional-metal (TM) oxides, such as Nb_2O_5, WO_3 or MoO_3 [3-5] due to the fact, that the high electrostatic field strength (z/a^2) of P^{5+} allows incorporating a high amount of TM oxides in phosphate glasses, in comparison to silicate glasses [1].

Phosphate glasses containing a high amount of niobium oxide exhibit non-linear optical properties, which make them attractive for various optical devices [6]. Niobophosphate glasses were considered also as potential candidates for the immobilization of nuclear wastes due to their low dissolution rates [7, 8]. The incorporation of large amount of Nb_2O_5 into phosphate glasses needs the addition of stronger bases of the 1st group (alkali oxides) or the 2nd group (alkaline earth oxides) [9]. Vitrification has been selected in various countries as the process for immobilizing high-level waste arising from reprocessing spent fuel. Some high-level solutions generated by reprocessing legacy fuel contain high molybdenum concentrations. Molybdenum oxide is known to be barely soluble in conventional borosilicate glass, and thus some studies have searched for suitable glass formulations for such waste [10]. Several previous studies [11-15] have reported the relatively high solubility of molybdenum oxide MoO_3 in phosphate glasses.

The aim of this work was to prepare and study phosphate and borophosphate glasses in systems $BaO\text{-}B_2O_3\text{-}P_2O_5$, $BaO\text{-}Nb_2O_5\text{-}B_2O_3\text{-}P_2O_5$, $BaO\text{-}Nb_2O_5\text{-}P_2O_5$ and $BaO\text{-}MoO_3\text{-}P_2O_5$ to determine their physico-chemical and thermal properties

and to investigate their structure. One of the main goals was also to find relationships between structure and properties of these glasses.

2. Experimental

The studied glasses were prepared by melting analytical grade $BaCO_3$, Nb_2O_5, MoO_3, H_3PO_4 and H_3BO_3 using a total batch weight of 20 g. The homogenized starting mixtures were slowly calcined up to 600°C and held at this temperature for 2 hrs in order to remove water. The reaction mixtures were then melted in a temperature range 900-1150°C under ambient air, in a platinum crucible. The melt was subsequently poured into a preheated graphite mould and the obtained glasses were then cooled to room temperature. The amorphous character of the prepared glasses was checked by X-ray diffraction analysis.

Density of glasses was measured using Archimedes` method. The molar volume (V_M) was calculated as $V_M = \overline{M}/\rho$, where $\overline{M}$ is the average molar weight of the glass composition. Chemical durability of the glasses was evaluated from the dissolution rate of the glass cubes in the distilled water at room temperature. The linear refractive indices were measured by the prism coupling method using a Metricon Model 2010/M.

Thermal behavior of the glasses was studied with a Netzsch DTA 404 over the temperature interval 30-1000°C. The measurements were carried out with 100 mg powder samples (the average particle size was 10 μm) in a silica crucible under an inert atmosphere of N_2. The thermal expansion coefficient, α, the glass transition temperature, T_g, and the dilatometric softening temperature, T_d, were determined on bulk samples with dimensions of 20×5×5 mm using a dilatometer DIL 402 PC (Netzsch) and a heating rate 5°C min^{-1}. The thermal properties were also studied with hot stage microscopy (HSM, from HESSE Gmbh) which was carried out with powder samples pressed into cylinders (3 mm in diameter and height) by a hand press.

ESR spectra of roughly crushed glassy samples were measured at ambient temperature at X-band (~ 9.5 GHz) using an ERS spectrometer. A microwave power of 10 mW, sufficiently below the saturation power, was used. Raman spectra were measured on bulk samples at room temperature using Horiba Jobin Yvon LabRam HR spectrometer. The spectra were recorded in back-scattering geometry under excitation with Nd-YAG laser radiation (532 nm) at a power of 12 mW. The spectral slit width was 1 mm, exposure time was 3s and accumulation number was 10.

^{31}P MAS NMR spectra were measured at 9.4 T on a BRUKER Advance 400 spectrometer with a 4 mm probe. The spinning speed was 12.5 kHz and relaxation (recycling) delay was 180s. The chemical shifts of ^{31}P nuclei are given relative to H_3PO_4 at 0 ppm. ^{11}B MAS NMR spectra were measured at 18.8 T on a BRUKER Avance 800 spectrometer with a 2.5 mm probe. The ^{93}Nb spectra were recorded at 18.8 T on a BRUKER Advance 800 spectrometer with a 3.2 mm probe. The spinning rate was 15 kHz. MAS spectra were recorded as echoes, with 1 s repetition time. The first pulse was 0.8 μs, the second 0.8 μs and the delay between the pulses was 0.2 s. $LiNbO_3$ was used as a secondary chemical shift reference (δ = -1025 ppm).

A Bruker D8 Advance diffractometer and CuK_α radiation was used for the identification of crystalline phases. A database of inorganic compounds from International Center of Diffraction Data [16] was used for the phase identification.

3. Results and discussion

3.1. Ternary BaO-B_2O_3-P_2O_5 glasses

Glasses of the ternary system BaO–B_2O_3–P_2O_5 were prepared and studied in broad concentration limits covering the whole vitrification domain. Altogether 14 glass samples were prepared in four compositional series A: $(100\text{-}x)Ba(PO_3)_2$-xB_2O_3, B: $40BaO$-yB_2O_3-$(60\text{-}y)P_2O_5$, C: $(50\text{-}z)BaO$-zB_2O_3-$50P_2O_5$ and

D: (60-w)BaO-wB_2O_3-40P_2O_5 in order to investigate the effect of composition on the structure and properties of these glasses. Their composition is shown in the ternary diagram in Fig. 1 with the glass forming region in this ternary system. All the prepared glasses were clean and homogeneous.

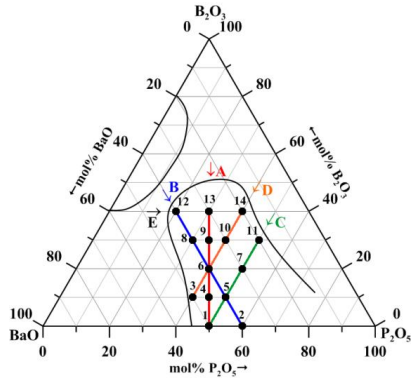

Fig. 1 *Phase diagram of the BaO-B_2O_3-P_2O_5 system with the glass forming region and the studied glasses.*

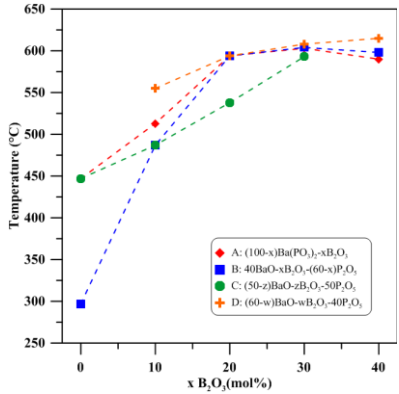

Fig. 2 *Compositional dependence of the glass transition temperature on B_2O_3 content. The lines are only a guide for the eye.*

The compositional dependence of the glass transition temperature for all compositional series is given in figure 2. As shown in this figure, the additions of B_2O_3 increase substantially the glass transition temperature in all series. T_g reaches

its maximum for the glasses containing 20-30 mol% (with the exception of series C). In these glasses the structural network is efficiently interlinked by P-O-B, P-O-P and B-O-B bridges into a three-dimensional structure [17] similarly to lead borophosphate glasses [18].

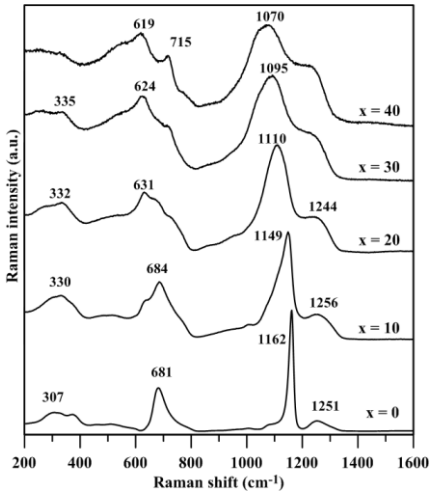

Fig. 3 *Raman spectra of (100-x)Ba(PO$_3$)$_2$-xB$_2$O$_3$ glasses.*

Raman spectra of the (100-x)Ba(PO$_3$)$_2$-xB$_2$O$_3$ glass series are shown in Fig. 3. The Raman spectrum of the starting barium metaphosphate glass is characterized by two strong vibrational bands at 1162 and 681 cm^{-1}. The first one is ascribed to the symmetric stretching vibration of the non-bridging phosphorus-oxygen bonds in metaphosphate Q^2 units [19] and its position is in a good agreement with the data of Nelson and Exarhos [20]. The band at 681 cm^{-1} is ascribed to the symmetrical stretching vibration of oxygen atoms in P-O-P chains in the barium metaphosphate glass structure. With an increasing B$_2$O$_3$ content in this glass series the band of 1162 cm^{-1} shifts to lower wavelengths up to 1070 cm^{-1} at the glass with x = 40 mol% B$_2$O$_3$ due to the shortening of phosphate chains by the incorporation of borate groups into phosphate chains. The vibrational band of 681 cm^{-1} with

increasing B_2O_3 content splits into two medium vibrational bands at 619 and 715 cm^{-1} on the Raman spectrum of the glass with x = 40. The band at 619 cm^{-1} could be ascribed to P-O-B stretching vibration, whereas the band at 715 cm^{-1} can be ascribed to the vibration of bridging oxygen atoms in P-O-P linkages of Q^1 diphosphate units. The other possibility is to ascribe the band of 715 cm^{-1} to the ring breathing vibrations of sixth-membered rings containing a trigonal boron and two BO_4 units like in paper [21] in sodium borophosphate glasses.

3.2. Quaternary $BaO-B_2O_3-Nb_2O_5-P_2O_5$ glasses

Fifteen homogeneous glass samples from the system $BaO-B_2O_3-P_2O_5-Nb_2O_5$ were prepared in two series A: $(100-x)[0.5BaO-0.1B_2O_3-0.4P_2O_5]-xNb_2O_5$ with x = 0-45 mol% Nb_2O_5 and B: $80[0.5BaO-yB_2O_3-(0.5-y)P_2O_5]-20Nb_2O_5$ with y = 0-0.25 B_2O_3. Glasses with $x \geq 20$ mol% Nb_2O_5 were blue colored and the color intensity increased with increasing Nb_2O_5 content. This blue color is caused by the presence of some amount of Nb^{4+} [6].

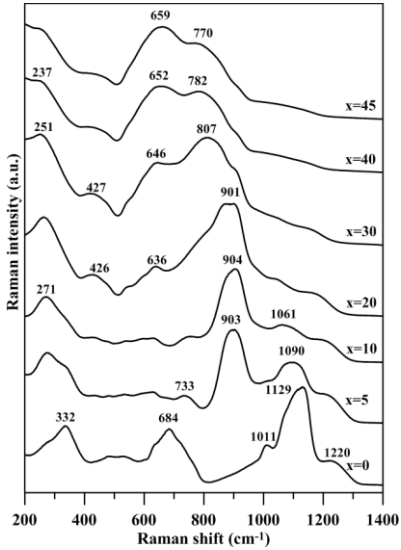

Fig. 4 *Raman spectra of $(100-x)[0.5BaO-0.1B_2O_3-0.4P_2O_5]-xNb_2O_5$ glasses.*

Raman spectra of the glass series A: (100-x)[0.5BaO-0.1B_2O_3-0.4P_2O_5]-xNb_2O_5 are shown in Fig. 4. Raman spectra of the starting 50BaO-10B_2O_3-40P_2O_5 borophosphate glass shows one dominant broad band in the high-frequency region with a maximum at 1129 cm^{-1} ascribed to the symmetric stretching vibration of non-bridging phosphate-oxygen bonds in PO_4 units [22]. The band at 684 cm^{-1} is due to the stretching vibration of P-O-P bonds in phosphate chains and the band at 332 cm^{-1} can be ascribed to the bending vibration of phosphate structural units. The vibrational band of phosphate units shifts to 1090 cm^{-1} for the glass with 5 mol% Nb_2O_5 and a new strong band at around 900 cm^{-1} appears in its Raman spectrum, which dominates on the Raman spectra within the compositional region of x = 5-20 mol% Nb_2O_5. This dominant band was ascribed by Cardinal et al. [6] to the stretching vibration of the Nb-O short bond in the isolated and distorted NbO_6 octahedra. We ascribed a new band at 273 cm^{-1} to deformation vibrations of NbO_6 octahedra. As the niobate units are very strong Raman scatterers in comparison with PO_4 groups, they suppress vibrational bands of phosphate units and thus no information on phosphate units can be obtained from Raman spectra of glasses with $x \geq 20$ mol% Nb_2O_5. For the Raman spectra of glasses containing x = 25-35 mol% Nb_2O_5, a broad vibrational band 799-853 cm^{-1} begins to dominate the spectra. This band is ascribed to the Nb-O-Nb vibration in the chains from NbO_6 octahedra interconnected by their corners [6]. Raman spectra of glasses with x = 40-45 mol% Nb_2O_5 are dominated by the broad band at 652-659 cm^{-1} ascribed to the Nb-O-Nb vibrations of NbO_6 octahedra in three-dimensional clusters [6].

^{11}B MAS NMR spectra of the series A: (100-x)[0.5BaO-0.1B_2O_3-0.4P_2O_5]-xNb_2O_5 are shown in Fig. 5. The starting barium borophosphate glass reveals two signals: the stronger one at -2.7 ppm and the weaker one at -0.9 ppm, which forms a shoulder on the left side of the stronger signal. The first resonance at – 2.7 ppm is ascribed to tetrahedral BO_4 units with B-O-P bonds [23, 24], whereas the second resonance at -0.9 ppm is ascribed to B^{IV}-O-B^{IV} bonds, because there are no BO_3

units present for the formation of B^{IV}-O-B^{III} bonds. Elbers et al. [24] from NMR experiments on silver borophosphate glasses came to the conclusion that no $B(OP)_4$ units are formed in borophosphate glasses and BO_4 units are involved in only three B-O-P linkages. These units may dimerize forming a diborate-type structure with BO^{IV}-BO^{IV} connectivity. Moreover, from these measurements the authors [24] concluded that BO_3 units do not form B-O-P bonds and form only B-O-B bonds. As we do not suppose the formation of covalent B-O-Ba bonds, we are convinced that the only possible assignments of the resonance at -0.9 ppm in Fig.7 is to the $B(OP)_2O_2$ tetrahedral units with one B-O-B bond. With an increasing Nb_2O_5 content, the intensity of the signal with the chemical shift δ = -0.9 ppm increases, while the intensity of the signal at -2.7 ppm decreases. NMR spectrum of the glass with x = 10 also reveals another resonance peaking at +13.2 ppm which is ascribed to trigonal BO_3 structural units [23]. Its intensity increases with increasing Nb_2O_5 content and its maximum gradually shifts up to +14.4 ppm.

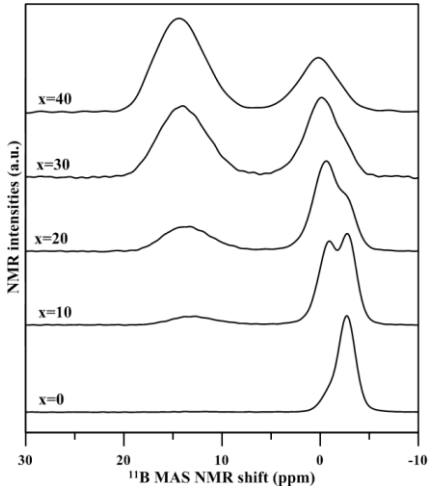

Fig. 5 *^{11}B MAS NMR spectra of (100-x)[0.5BaO-0.1B_2O_3-0.4P_2O_5]-xNb_2O_5 glasses.*

Fig. 6 shows the ^{93}Nb static-NMR spectra of the (100-x)[0.5BaO-0.1B_2O_3-0.4P_2O_5]-xNb_2O_5 glasses. Former works on sodium niobiophosphate glasses [25] indicated chemical shifts ranges from -1000 to -1250 ppm for corner or edge-shared NbO_6 groups, and -1300 to -1650 ppm for mixed phosphate-niobate units. As can be seen on figure 10, the static ^{93}Nb spectra are non-symmetric at low Nb content and become more symmetric with increasing content of Nb_2O_5 in the glasses. This indicates that the local environment of niobium atoms becomes more regular. This is in agreement with the presence of symmetric NbO_6 units, like those reported in sodium niobophosphate glasses [25]. In our glasses, the presence of barium instead of sodium induces a larger width of the resonances, probably due to larger distributions of local environment that contribute to an increase of the chemical shift anisotropy and the quadrupolar parameters.

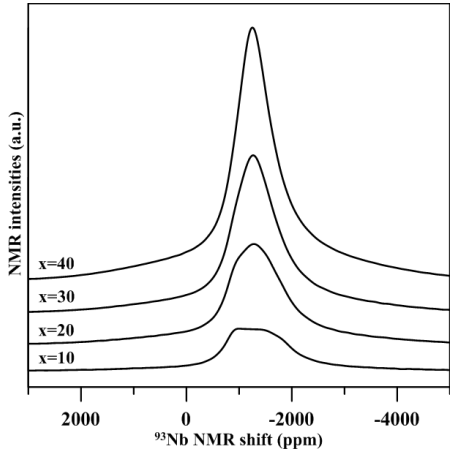

Fig. 6 *^{93}Nb static-NMR spectra of the (100-x)[0.5BaO-0.1B_2O_3-0.4P_2O_5]-xNb_2O_5 glasses.*

3.3. Ternary BaO-Nb_2O_5-P_2O_5 glasses

Nine homogeneous glass samples from the system BaO-P_2O_5-Nb_2O_5 were prepared in this study in two compositional series A: 40BaO-xNb_2O_5-(60-x)P_2O_5,

with x = 0-40 mol% Nb_2O_5, and B: yBaO-20Nb_2O_5-(80-y)P_2O_5, with y = 20-60 mol% BaO. Two glasses from the second series, with contents of 50 and 60 mol% P_2O_5, were deep-blue in color, thus suggesting the presence of some Nb^{4+} ions, whereas the other glasses were clear or slightly yellow.

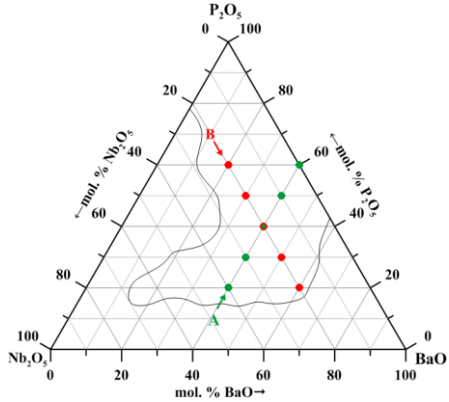

Fig. 7 *Phase diagram of the BaO-Nb_2O_5-P_2O_5 system with the glass forming region and the studied glasses.*

The compositional dependences of glass transition temperature T_g, dilatometric softening temperature T_d and the thermal expansion coefficient, α, for glasses in the first compositional series 40BaO-xNb_2O_5-(60-x)P_2O_5 are given in Fig. 8. The T_g and T_d values increase steeply within the range 0-20 mol%, reaching their maxima at about 30 mol% Nb_2O_5. The thermal expansion coefficient, in the presence of increasing Nb_2O_5 content, rapidly decreases from 14.5 ppm $°C^{-1}$ down to its minimum at 8.0 ppm $°C^{-1}$ at the glass with 30 mol% Nb_2O_5. The reason for the observed steep increase in T_g and T_d can be ascribed to several factors. The most important are the cross-link density of the network and the strength of chemical bonds [26]. The first reason for this increase in the studied glasses is the formation of Nb-O-P bonds as a result of the incorporation of Nb_2O_5 into the phosphate network.

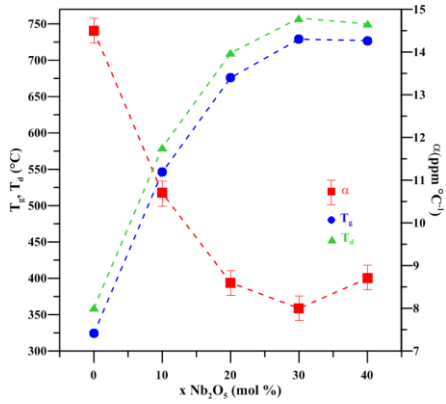

Fig. 8 *Compositional dependence of glass transition temperature T_g, dilatometric softening temperature T_d, thermal expansion coefficient, α, in the glass series A: 40BaO-xNb_2O_5-(60-x)P_2O_5 on the Nb_2O_5 content. The error in the values of T_g and T_d is smaller than the symbol size. The lines are only a guide to the eye.*

When niobium oxide is added to phosphate glasses, NbO_6 polyhedra interconnects the phosphate chain by Nb-O-P bonds, which increase the cross-link density and thus increases T_g and decreases thermal expansion coefficient [27]. The second reason for an increase in T_g and T_d in the first glass series are the differences in the energy of P-O and Nb-O bonds. The formation of stronger Nb-O bonds (E_{Nb-O} = 771.5 kJ/mol [28]), replacing weaker P-O bonds (E_{P-O} = 599.1 kJ/mol [28]) in the glass structure, contributes to the observed steep increase of T_g in the first compositional series A: 40BaO-xNb_2O_5-(60-x)P_2O_5. A weaker increase of T_g within the x = 20-40 mol% Nb_2O_5 region can be explained by the fact that glass network reticulation reaches its maximum at about 20-30 mol% Nb_2O_5 and that the clustering of NbO_6 octahedra above 20 mol% Nb_2O_5 means the formation of nano-heterogeneous regions within the niobophosphate network.

The compositional dependence of linear refractive index, n_d, is given in Fig. 9 for both compositional series. From this figure it is evident that in series

A 40BaO-xNb_2O_5-(60-x)P_2O_5, with a constant BaO content, the index of refraction increases more steeply with increasing Nb_2O_5 content than in series B yBaO-20Nb_2O_5-(80-y)P_2O_5 with increased BaO content. It is evident that the main role in the optical properties of the studied glasses is played by the number of Nb-O ions, which make a substantial contribution to the molecular refractive index of barium niobophosphate glasses [7]. On the other hand, an increasing amount of heavy Ba atoms with high electron density also contribute significantly to the molecular refractive index of glasses in the B series.

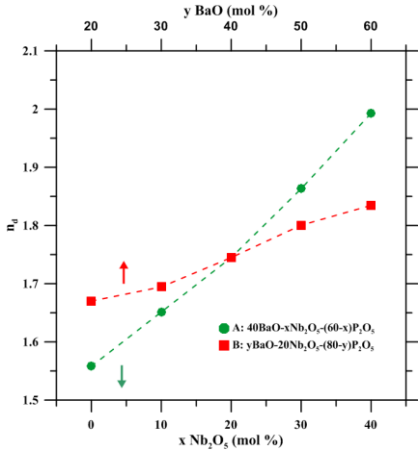

Fig. 9 *Compositional dependence of the index of refraction of glass series A: 40BaO-xNb_2O_5-(60-x)P_2O_5 and B: yBaO-20Nb_2O_5-(80-y)P_2O_5. The error in the values of n_d is smaller than the symbol size. The lines are only a guide to the eye.*

Study of the glass to crystal transformation was realized for two ternary compounds belonging to the glass-forming region of the BaO-Nb_2O_5-P_2O_5 system: $Ba_3Nb_2(PO_4)_4O_2$ with 16.66 mol% Nb_2O_5 (glass composition 3BaO.1Nb_2O_5.2P_2O_5, marked as (312)) and $BaNb_2P_2O_{11}$ with 33.33 mol% Nb_2O_5 (glass composition 1BaO.1Nb_2O_5.1P_2O_5, marked as (111)). The Raman spectra of (312) and (111) glasses are shown in Fig. 10. Raman spectrum of the (312) glass contains a broad dominant vibrational band peaking at 873 cm^{-1}. Its position lies between the

position of vibrations of short Nb-O bonds in isolated NbO_6 octahedra at ~900 cm^{-1} [6] and the position of vibrational band of bridging oxygen atoms in Nb-O-Nb chains connecting corners of NbO_6 octahedra at ~800 cm^{-1} [6].

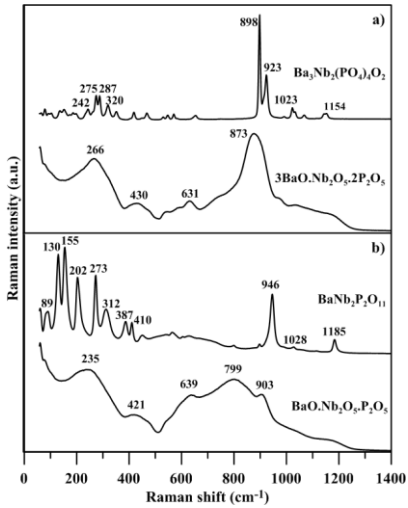

Fig. 10 *Raman spectra of the $3BaO.Nb_2O_5.2P_2O_5$ glass and the corresponding polycrystalline compound $Ba_3Nb_2(PO_4)_4O_2$ (a) and $BaO.Nb_2O_5.P_2O_5$ glass and the corresponding polycrystalline compound $BaNb_2P_2O_{11}$ (b).*

The second strong band at 266 cm^{-1} probably belongs to deformation vibrations of NbO_6 octahedra [6]. Raman spectrum of the (111) glass contains a broad complex band within the range of 500-1000 cm^{-1}, composed of three sub bands peaking at 639, 799 and 903 cm^{-1}. These bands show the presence of a small amount of "isolated" NbO_6 octahedra (band at 903 cm^{-1}), some NbO_6 octahedra interconnected via Nb-O-Nb bridges (band at 799 cm^{-1}) and a small amount of 3D-clusters formed from NbO_6 octahedra connected by edges (band 639 cm^{-1} [6]).

3.4. Ternary $BaO-MoO_3-P_2O_5$ glasses

Molybdenum oxide is able to form phosphate glasses within a broad concentration range. 24 homogeneous glass samples from the ternary system

BaO-MoO_3-P_2O_5 were prepared in this study in four compositional series A: (100-x)[0.5BaO-0.5P_2O_5]-xMoO_3, B: 50BaO-yMoO_3-(50-y)P_2O_5, C: 20BaO-zMoO_3-(80-y)P_2O_5 and D: (70-u)BaO-zMoO_3-30P_2O_5. Glass samples containing MoO_3 were green in color, thereby showing the presence of Mo^{+5} species in the glasses, which was confirmed by ESR spectroscopy. The ESR studies also showed that the ratio of Mo^{+V}/ Mo^{total} was mostly below 2%.

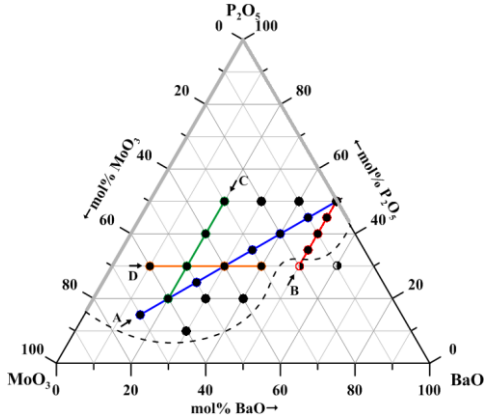

Fig. 11 *Phase diagram of the BaO-MoO_3-P_2O_5 system with the glass forming region and the studied glasses.*

Raman spectra of the glass series A are shown in Fig. 12. The spectrum of barium metaphosphate glass is characterized by the dominant band at 1161 cm^{-1} (symmetrical stretching vibration of non-bridging oxygen atoms in Q^2 units [19]) and the medium band at 680 cm^{-1} (symmetrical stretching vibration of bridging oxygen atoms between Q^2 units [19]). With the additions of MoO_3, two strong vibrational bands appear in the Raman spectra at 944 and 900 cm^{-1}, ascribed to the vibration of Mo-O^- and M=O bonds in the molybdate structural units [11]. Characteristic spectral features of phosphate units decrease in intensity with increasing MoO_3 content, due to a much higher Raman scattering efficiency for Mo-O vibrations than for P-O vibrations [16], and thus no vibrational bands of

phosphate units can be seen in the Raman spectra of glasses with 30-70 mol% MoO_3. In the Raman spectra of glasses with 40-70 mol% MoO_3 a broad band at 853-854 cm^{-1} increases in strength when MoO_3 content increases. This band can be ascribed to the vibration of Mo-O-Mo bonds interconnecting MoO_6 octahedra [13]. A small vibrational band at 390-394 cm^{-1}, which is present only in the spectra of molybdate-phosphate glasses, is ascribed to the vibrations of Mo-O-P bonds [15].

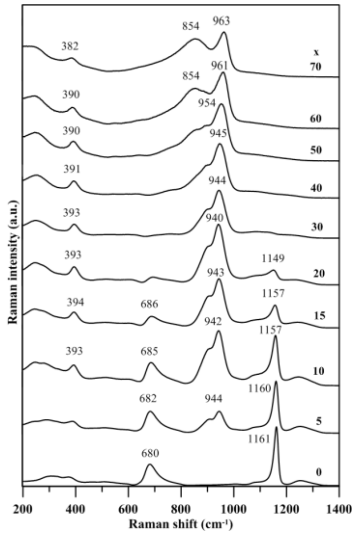

Fig. 12 *Raman spectra of A: (50-x/2)BaO-xMoO_3-(50-x/2)P_2O_5.*

^{31}P MAS NMR spectra of the glass series A: (100-x)[0.5BaO-0.5P_2O_5]-xMoO_3 are shown in Fig. 13. The NMR spectrum of barium metaphosphate glass (x = 0) is characterized by the dominant signal of Q^2 units with the chemical shift δ = -24.7 ppm. A small contribution of Q^1 resonance at -8.8 ppm (3%) shows the presence of a few terminal Q^1 units at the ends of metaphosphate chains. By fitting the NMR spectra we obtained characteristic parameters of the decomposed spectra, graphically presented in Fig. 14. With the additions of MoO_3 to the parent barium metaphosphate glass, the depolymerization of phosphate chains takes place, as

revealed by the increasing intensity of the signal of Q^1 units up to the glass with x = 30 mol% MoO_3, where these units reach its maximum value of 74% and then their amount in the glass structure decreases. The first appearance of the signal of Q^0 units at -4.2 ppm starts with the 40 mol% MoO_3 glass and then their amount steadily increases up to the glass with 70 mol% MoO_3, where these units dominate in the glass structure with 96 %.

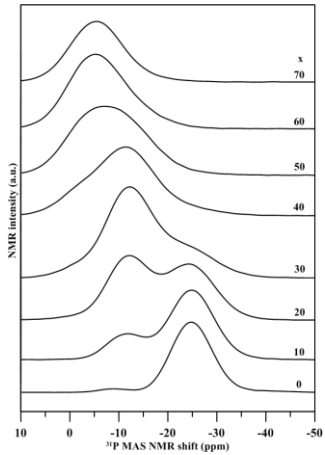

Fig. 13 *^{31}P MAS NMR spectra of glass series A: (50-x/2)BaO-xMoO_3-(50-x/2)P_2O_5.*

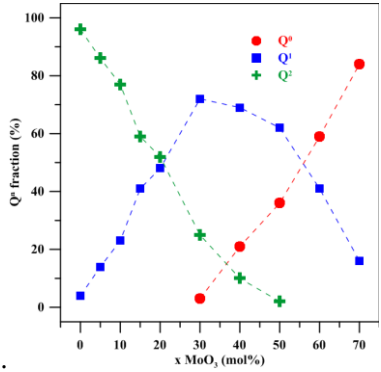

Fig. 14 *Compositional dependences of the relative amounts of phosphate structural units in the glass series A obtained from the decomposition of their ^{31}P MAS NMR spectra. The lines are only a guide for the eye.*

This study also revealed the formation of the compound $Ba(MoO_2)_2(PO_4)_2$ in this ternary system by annealing glass powder of the sample with composition $25BaO\text{-}50MoO_3\text{-}25P_2O_5$ for 3 hrs on temperatures above its crystallization peak on DTA curve. For this composition, differential thermal analysis has been used also for the study of the dominant crystallization mechanism by the method of Ray and Day [30]. The mechanism of crystallization (surface or internal) was evaluated from the changes of the shape and position of the crystallization peak on DTA curves in the dependence on the particle size (130, 300, 600 and 900 μm) of the studied glasses (Fig. 15). With increasing grain size of the sample the crystallization peak shifts to higher temperature and its height is decreasing, meanwhile the width of the peak is increasing. This behavior is according to [30] typical for surface crystallization.

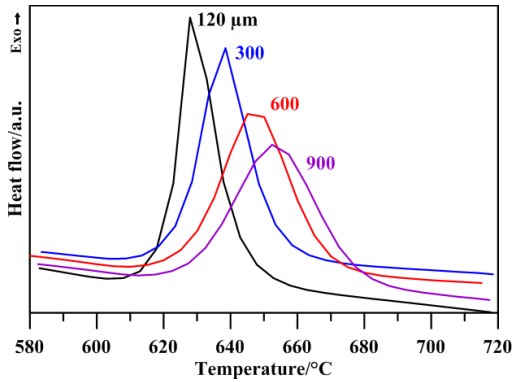

Fig. 15 *The change of the crystallization peaks for $25BaO\text{-}50MoO_3\text{-}25P_2O_5$ glass depending on the grain size of the sample.*

4. Conclusion

This dissertation summarizes the results of investigation of barium phosphate and borophosphate glasses in the systems $BaO–B_2O_3–P_2O_5$, $BaO–B_2O_3–Nb_2O_5\text{-}P_2O_5$, $BaO\text{-}Nb_2O_5\text{-}P_2O_5$ and $BaO\text{-}MoO_3\text{-}P_2O_5$. The aim of this dissertation was the

preparation and study of these glasses, mostly of the original compositions, the examination of their physico-chemical and thermal properties, the study of their structure and interpretation of the relationships between the structure and properties of glasses.

For structural studies the combination of Raman and NMR spectroscopy was applied. The modification of barium phosphate and borophosphate glasses with niobium oxide increases chemical durability and substantially increases the index of refraction of the glasses. At low Nb_2O_5 content niobium forms isolated NbO_6 octahedra incorporated in the glass network, but when Nb_2O_5 content increases, these octahedra are linked into chains through Nb-O-Nb bonds and further into three-dimensional clusters.

Molybdenum oxide forms large glass-forming region with barium phosphates and glasses with a high content of 70 mol% MoO_3 can be prepared as well as with only 10 mol% P_2O_5. Phosphate glasses with MoO_3 at low MoO_3 content contain isolated MoO_6 octahedra. At high MoO_3 content, these octahedra are interconnected through Mo-O-Mo bonds. In glasses with a low P_2O_5 content the formation of MoO_4 units cannot be excluded.

5. References

[1] J.R. van Wazer, Phosphorus and Its Compounds, vol. 1, Interscience, New York, 1958.
[2] R.K. Brow, J. Non-Cryst. Solids 263&264 (2000) 1-28.
[3] L. Koudelka, P. Kalenda, P. Mošner, L. Montagne, B. Revel, J. Non-Cryst. Solids. 437 (2016) 64-71.
[4] S.H. Santagneli, C.C. de Araujo, W. Strojek, H. Eckert, G. Poirier, S.J.L. Ribeiro, Y. Messaddeq, J. Phys. Chem. B. 111 (2007) 101-109.
[5] C.C. de Araujo, W. Strojek, L. Zhang, H. Eckert, G. Poirier,S. J. L. Riberio, Y. Messaddeq, J. Mater. Chem. 16 (2006) 3277-3284.
[6] T. Cardinal, E. Fargin, G. Le Flem, M. Couzi, L. Canioni, P. Segonds, L. Sarger, A. Ducasse, F. Adamietz, Eur. J. Solid State Inorg. Chem., 33 (1996) 597-605.
[7] L. Ghussn, J.R. Martinelli, J. Mater. Sci. 39 (2004) 1371-1376.
[8] L. Ghussn, M.O. Prado, D.O. Russo, J.R. Martinelli, J. Non-Cryst. Solids 352 (2006) 3391-3397.
[9] L. Koudelka, J. Pospíšil, P. Mošner, L. Montagne, L. Delevoye, J. Non-Cryst. Solids, 354 (2008) 129-133.
[10] O. Pinet, J.L. Dussossoy, C. David, C. Fillet, J. Nucl. Mater. 377 (2008) 307-312.
[11] B.V.R. Chowdari, R. Gopalakrishan, S.H. Tang and M.H. Kuok, Solid State Ionics 28-30 (1988) 704-709.
[12] B.V.R. Chowdari, K.L.Tan, W.T. Chia, Mater. Res. Soc. Symp. Proc. Vol. 293 (1993) 325-336.
[13] S.H. Santagneli, C.C. de Araujo, W. Strojek, H. Eckert, G. Poirier, S.J.L. Ribeiro, Y. Messaddeq, J. Phys. Chem. B 111 (2007) 10109-10117.
[14] J. Šubčík, L. Koudelka, P. Mošner, L. Montagne, G. Tricot, I. Gregora, J. Non-Cryst. Solids 356 (2010) 2509-2516.
[15] L. Koudelka, I. Rosslerová, J. Holubová, P. Mošner, L. Montagne, J. Non-Cryst. Solids 357 (2011) 2816-2821.
[16] Joint Committee on powder diffraction standards, Swarthmore, PA, USA. International Centre of Diffraction Data.
[17] L. Koudelka, P. Kalenda, P. Mošner, Z. Černošek, L. Montagne, B. Revel. J. Mol Struct. 1119 (2016) 212-219.
[18] Koudelka L, Mošner P, Zeyer M, Jäger C, Phys Chem Glasses. 43C (2002) 102-107.
[19] Ya. S. Bobovich, Opt. Spektrosk. 13 (1962) 492-497.
[20] B.N. Nelson, G.J. Exarhos, J. Chem. Phys. 71 (1979) 2739-2747.
[21] R. Christensen, G. Olson, W.W. Martin, J. Phys. Chem B 117 (2013) 2169-2179.

[22] L. Koudelka, P. Mošner, M. Zeyer, C. Jäger, Phys. Chem. Glasses 43C (2002) 102–107.
[23] R.K. Brow, D. Tallant, J. Non-Cryst. Solids 222 (1997) 396-406.
[24] S. Elbers, W. Strojek, L. Koudelka, H. Eckert, Solid State Nucl Magn Resonance 27 (2005) 65-76.
[25] A.Flambard, L. Montagne, L. Delevoye, G. Palavit, J.P. Amoureux, J.J.Videau, J. Non-Cryst. Solids 345&346 (2004) 75-79.
[26] N.H. Ray, J. Non-Cryst. Solids, 15 (1974) 423-434.
[27] S.M. Hsu, J.J. Wu, S.W. Yung, T.S. Chin, T. Zhang, Y.M. Lee, C.M. Chu, J.Y. Ding, J. Non-Cryst. Solids 358 (2012) 14-19.
[28] D.R. Lide, Handbook of Chemistry and Physics CRC Press, Boca Raton (2001)
[29] F.F. Sene, J.R. Martinelli, L. Gomes, J. Non-Cryst. Solids 348 (2004) 30-37.
[30] C. S. Ray, D. E. Day, Thermochim. Acta. 280-281 (1996) 163-174.

List of published articles:

Articles related to presented dissertation

1. P. Kalenda, L. Koudelka, P. Mošner, L. Beneš, Thermal behavior and the properties of $BaO-B_2O_3-P_2O_5$ glasses, J. Therm. Anal. Calorim., 124 (2016) 1161-1168.
2. L. Koudelka, P. Kalenda, P. Mošner, Z. Černošek, L. Montagne, B. Revel, Structural investigation of $BaO-B_2O_3-P_2O_5$ glasses by NMR and Raman spectroscopy, J. Mol. Struct., 1119 (2016) 212.-219.
3. L. Koudelka, P. Kalenda, P. Mošner, L. Montagne, B. Revel, Structure-property relationships in barium borophosphate glasses modified with niobium oxide, J. Non-Cryst. Solids, 437 (2016) 64-71.
4. L. Koudelka, P. Kalenda, P. Mošner, L. Montagne, B. Revel, Structure and properties of barium niobophosphate glasses, J. Non-Cryst. Solids 459 (2017) 68-74.
5. P. Kalenda, L. Koudelka, P. Mošner, L. Montagne, B. Revel, J. Trebosc, Glass to crystal transformation in the ternary $BaO-Nb_2O_5-P_2O_5$ system, J. Mol. Struct. 1143 (2017) 472-477.
6. L. Koudelka, P. Kalenda, J. Holubová, P. Mošner, L. Montagne, B. Revel, Structural study of $BaO-MoO_3-P_2O_5$ glasses by Raman and NMR spectroscopy, J. Non-Cryst. Solids 476 (2017) 114-121.
7. P. Kalenda, L. Koudelka, P. Mošner, L. Beneš, Z. Černošek, Thermal properties and crystallization of $BaO-MoO_3-P_2O_5$ glasses, J. Therm. Anal. Calorim. (submitted)

Other published articles

8. L. Koudelka, I. Rösslerová, P. Kalenda, P. Mošner, L. Montagne, B. Revel, Characterization and structural investigation of lead borophosphate glasses modified by tungsten oxide, J. Alloys Compd., 658 (2016) 377-384.
9. A. Moguš-Milanković, K. Sklepić, P. Mošner, L. Koudelka, P. Kalenda, Lithium-Ion Mobility in Quaternary Boro–Germano–Phosphate Glasses, J. Phys. Chem. B, 120 (2016) 3978-3987.

Presentations at conferences:

1. P. Kalenda, I. Rösslerová, L. Koudelka, Lead borophosphate glasses modified by tungsten oxide, Development of Materials Science in Research and Education, Lednice, 8. - 12.9 2014, Sborník str. 22, ISBN 978-80-260-6599-9. (oral presentation)
2. P. Kalenda, L. Koudelka, P. Mošner, Z. Černošek, Studium vlastností a struktury borofosfátových skel barnatých, 67. Zjazd chemikov, Vysoké Tatry, 7. – 11.9. 2015 (poster presentation)
3. P. Kalenda, L. Koudelka, Thermal properties and crystallization of alkaline-earth borophosphate glasses, XXI. ročník odborného semináře doktorandů „Anorganické nekovové materiály“, Praha, 10. - 11.2 2015, Sborník ANM 2015 str. 34. (oral presentation)
4. P. Kalenda, L. Koudelka, Borofosfátová skla olovnatá modifikovaná přídavky oxidu wolframového, Česká a slovenská konference o skle, Žďár nad Sázavou, 5. – 7.11 2014, str. 36, ISBN 978-80-7080-902-0 (poster presentation)
5. P. Kalenda, L. Koudelka, P. Mošner, Z. Černošek, Speciální optická skla na bázi borofosfátů barnatých, 3. mezinárodní chemicko-technologická konference, Mikulov, 13. – 15.4. 2015, p.14., ISBN 978-80-86238-79-1 (poster presentation)
6. P. Kalenda, L. Koudelka, Characterization and structural investigation of lead borophosphate glasses modified by tungsten oxide, XX. workshop of PhD students „Inorganic non-metallic materials“, Prague, 10. - 11.2 2016, Sborník ANM 2016 str. 6. (oral presentation)
7. P. Kalenda, L. Koudelka, P. Mošner, L. Montagne, B. Revel, $BaO\text{-}Nb_2O_5\text{-}P_2O_5$ glasses and their crystallization, SGT Centenary conference & ESG 2016, Sheffield UK, 4. – 8.9. 2016. (poster presentation)
8. P. Kalenda, L. Koudelka, P. Mošner, L. Montagne, B. Revel, Investigation of barium borophosphate glasses modified with niobium oxide, Solid state chemistry, Praha, 18. – 23.9. 2016. (poster presentation)
9. P. Kalenda, L. Koudelka, P. Mošner, A. Moguš-Milanković, K. Sklepić, Mixed alkali effect in lithium-sodium phosphate glasses modified with tungsten oxide, 5th International Conference on Chemical Technology, Mikulov, Czech Republic, 10.4.-12.4. 2017. (poster presentation)
10. P. Kalenda, L. Koudelka, P. Mošner, L. Montagne, B. Revel, P. Simon, Investigation of $BaO\text{-}Nb_2O_5\text{-}P_2O_5$ glasses, Slovak and Czech glass conference & seminar on defects in glass, Trenčianske Teplice, Slovakia, 28.6.-30.6. 2017, Sborník str. 40. (poster presentation)

11. P. Kalenda, L. Koudelka, P. Mošner, L. Montagne, B. Revel, Structure-property relationships in $BaO-Nb_2O_5-P_2O_5$ glasses, The 9th International Conference on Borate Glasses, Crystals and Melts and the 2nd International Conference on Phosphate Materials, Oxford, UK, 24.7.-28.7. 2017, Sborník str. 150. (poster presentation)